Available online at www.sciencedirect.com
ScienceDirect
Journal of the European Ceramic Society 27 (2007) 35–39
www.elsevier.com/locate/jeurceramsoc

The dependence of the elastic moduli of reaction bonded alumina on porosity

Stephan Puchegger [a], Frank Dose [b], Dieter Loidl [c], Karl Kromp [a], Rolf Janssen [b], D. Brandhuber [d], N. Hüsing [e], Herwig Peterlik [a,*]

[a] *Institute of Materials Physics, University of Vienna, Boltzmanngasse 5, A-1090 Vienna, Austria*
[b] *Department Technical Ceramics, Technical University Hamburg-Harburg, Denickestraße 15, D-21073 Hamburg, Germany*
[c] *Institute of Physics and Materials Science, University of Natural Resources and Applied Life Sciences, Peter-Jordan-Straße 82, A-1190 Vienna, Austria*
[d] *Institute of Materials Chemistry, Technical University of Vienna, Getreidemarkt 9/165, A-1060 Vienna, Austria*
[e] *Inorganic Chemistry I, University of Ulm, Albert Einstein Allee 11, D-89081 Ulm, Germany*

Received 19 November 2005; received in revised form 3 April 2006; accepted 21 April 2006
Available online 18 July 2006

Abstract

The resonant beam technique (RBT) allows the simultaneous determination of the Young's and the shear modulus. In the present paper this method is extended to materials covering an extremely wide range of porosities from nearly dense to the limit of stability, which is shown for ZrO_2-toughened reaction-bonded Al_2O_3 (RBAO) ceramics as an example. Additional characterisation of the pore structure and the material's composition was performed to exclude an influence of structural parameters other than porosity.

Keywords: Elastic moduli; Mechanical properties; RBAO; Porosity; Al_2O_3

1. Introduction

The demand for the saving of energy requires light-weight and highly porous materials with a significant strength and sufficiently high elastic moduli. Porous ceramics offer furthermore high temperature resistance, which is favourable for aerospace applications. For alumina, numerous works are therefore dealing with the porosity dependence of its elastic properties (see Ref. [1] for an overview). Most of the experimental methods reported in the literature are restricted to the dependence of the Young's modulus on the porosity, but also few data on both Young's and shear modulus are available.[2,3] Both the Young's and the shear modulus can be obtained by the resonant beam technique (RBT),[4–6] which uses the fundamental frequency and the higher modes of resonance. In the present paper, this method is extended to the measurement of the elastic moduli of materials covering an extremely wide range of porosities from nearly dense to the limit of stability, which is shown for ZrO_2-toughened reaction-bonded Al_2O_3 (RBAO) ceramics as an example. RBT has the same sample preparation and requirements as the resonant frequency technique described in the ASTM-standard,[7] but gives both the Young's and the shear modulus in one step. This is advantageous, if the properties of the material are permanently changed during the measurement, e.g. by a phase transition in the course of testing at elevated temperatures. The method is also applicable to determine anisotropic elastic properties,[5,6] which is difficult for torsion tests due to the complicated interaction of different shear moduli within the cross-section.

Among the different approaches to describe experimental data[1,8–16] four different models were chosen, the self-consistent scheme for two different pore geometries,[11–14] the dilute-distribution[15] and the differential model.[16] All four models are based on the so-called Eshelby tensor S_{ijkl},[17] which describes the effect of an ellipsoidal inclusion on the strain field of an elastic body.

The goal of this work is thus two-fold: the first is to show that RBT can be used to determine the elastic moduli of highly porous materials in one step and the second to document the elastic properties of the specific material RBAO in dependence on porosity.

* Corresponding author. Tel.: +43 1 4277 51350; fax: +43 1 4277 9513.
E-mail address: herwig.peterlik@univie.ac.at (H. Peterlik).

0955-2219/$ – see front matter © 2006 Elsevier Ltd. All rights reserved.
doi:10.1016/j.jeurceramsoc.2006.04.181

2. Material and experimental

2.1. Material and sample preparation

The material investigated in this work was a ZrO_2-toughened reaction bonded Al_2O_3 (RBAO). This material was originally developed by Claussen[18,19] and shows far better mechanical properties than pure Al_2O_3. The additional possibility to tailor the shape of the green-body makes this technique very attractive. The basic idea of RBAO is to heat treat attrition-milled Al/Al_2O_3-powder-compacts in air, so that Al oxidises to new Al_2O_3 crystallites, which bond the Al_2O_3 ceramic-particles during sintering. Reduced shrinkage and high strength are the main features of this type of Al_2O_3-based ceramics. To investigate the porosity dependence of the elastic moduli, specimens with different porosities were prepared: a 50 vol.% Al, 30 vol.% Al_2O_3 and 20 vol.% ZrO_2 powder mixture was wet milled in acetone in an attrition-mill for 7 h. The bowl of the attrition-mill consists of Al_2O_3, the milling media, and ZrO_2 spheres and discs. The milled powder was then dried for 2 days and finally sieved to remove agglomerates with diameters larger than 1 μm. The addition of ZrO_2 to the powder mixture results in ceramics with a much higher strength than pure Al_2O_3.[20]

The green compaction is a two-step process: the samples are first pressed uniaxially into a mould and then pressed a second time in a cold isostatic press. After the compaction, the green body has a homogeneous texture with particles smaller than 1 μm together with microporosity.

The samples were heated in an oxidizing atmosphere to temperatures above 350 °C and sintered at temperatures above 1135 °C. The composition of the material after the reaction bonding is 82.5 vol.% Al_2O_3 and 17.5 vol.% ZrO_2. After 10 min the first sample was removed from the sintering process, and every 5 min thereafter another sample was taken out of the furnace. The first sample removed is the one with the highest porosity. The porosity decreases with the time spent in the furnace, as the density increases in the course of the sintering process. Samples with porosities ranging from 0.053 to 0.45 pore volume fraction were obtained. The porosity was calculated from the ratio bulk density to theoretical density and additionally determined by the liquid displacement method.

2.2. Measurement of elastic moduli

For the dynamic method RBT,[5,6] a specimen (a beam with rectangular cross-section and an aspect ratio of approximately 10) is suspended in two carbon fibre loops. Both loops are attached to piezoelectric transducers. The specimen is excited to flexural vibrations by one of the transducers, while the other records the resonance frequencies via a network-analyser. The equipment allows the detection of even very weak resonances due to the low noise level of about −140 dBm.[a]

[a] dBm (decibels/milliwatt), technical definition: 0 dBm is defined as 1 mW at 1 kHz of frequency at 600 Ω of impedance.

The evaluation of RBT-measurements is based on Timoshenko's beam theory.[21,22] The evaluation procedure numerically solves an inverse problem, i.e., the elastic moduli are determined via minimising the difference between calculated and measured eigen frequencies.

The accuracy of the theory depends on the shear correction factor k, which takes the actual shear stress distribution in the beam cross-section into account. This correction factor has been audited experimentally[23] and theoretically[24] by comparison with results from resonant ultrasound spectroscopy.[25] With the appropriate choice for the shear correction factor, RBT and RUS give identical values for samples with the requirements listed in Ref. [7].

2.3. Material and pore characterisation

Wide-angle X-ray diffraction (WAXD) and small-angle scattering (SAXS) were performed using a rotating anode generator, a pinhole camera (Cu Kα-radiation) and an area detector (Bruker AXS Karlsruhe). The specimen to detector distances was 1.04 and 0.2 m for the SAXS and 0.043 m for the WAXS measurements, respectively. This allowed to cover a range of the scattering angle 2θ from 0.15° to 48°.

Nitrogen adsorption–desorption isotherms were determined at −196 °C using an adsorption porosimeter (NOVA 4000e Quantachrome). Samples were outgassed for 6 h in the degas unit at 200 °C prior to analysis. The BET surface area was evaluated using adsorption data in a relative pressure range from 0.05 to 0.2 (S^{BET}). The total pore volume was estimated from the amount adsorbed at a relative pressure of about 0.99.

2.4. Models for comparison of theory and experiment

Four models were used for the prediction of theory and experiment: (a) the self-consistent scheme, first used by Hill[11] and Budiansky,[12] estimates the overall elastic properties of a composite material by embedding a single inhomogeneity with the shape of an ellipsoid of revolution in an unbound homogeneous solid, (b) the self-consistent scheme for ellipsoids of revolution with a random angle distribution and a specific aspect ratio α,[13,14] (c) the dilute-distribution model[15] and (d) the differential model.[16] The models are quite elaborate and the reader is referred to the original papers for further information in the models. In this paper, fitting of the experimental data to Wu's model[13,14] was performed with Mathematica (Version 4.1, Wolfram Research) to obtain the porosity dependence of the Young's modulus, the shear modulus and the aspect ratio α. The zero porosity values were then used to calculate the predictions from the other theories.

3. Results

The experimental results from the measurement of the Young's and the shear modulus are depicted in Figs. 1 and 2. The Poisson ratio ν of the different samples in Fig. 3 was calculated from the Young's and the shear modulus, $\nu = E/(2G) - 1$.

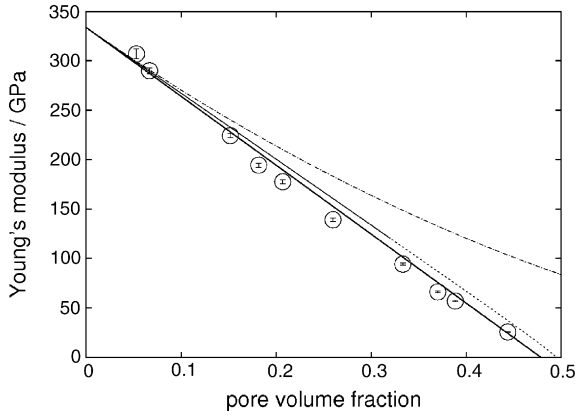

Fig. 1. The Young's modulus vs. the pore volume fraction (error bars showing the standard error of RBT). Dilute-distribution model (dotted line), differential model (dashed-dotted line), spherical self-consistent scheme (solid line) and Wu's theory (bold solid line).

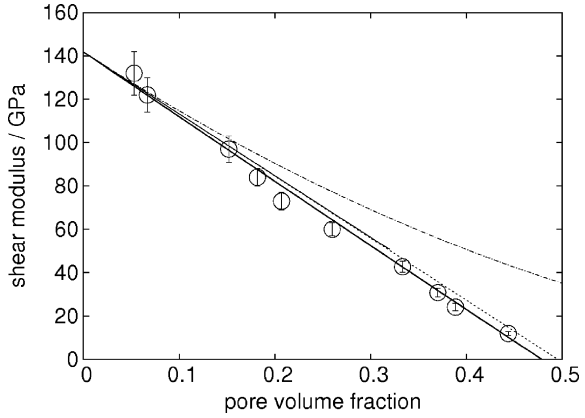

Fig. 2. The shear modulus vs. the pore volume fraction (error bars showing the standard error of RBT). Symbols and lines are the same as in Fig. 1.

The prediction of the four theories for the respective moduli in dependence on the porosity is also included in all three figures.

The fit for the theoretical values for the Young's modulus, the shear modulus and the pore aspect ratio $\alpha = a/c$ resulted in the values $E_M = 334$ GPa and $G_M = 142$ GPa for pore volume fraction 0 as well as $\alpha = 0.61$ – lenticular pores, which are nearly half as high as they are wide.

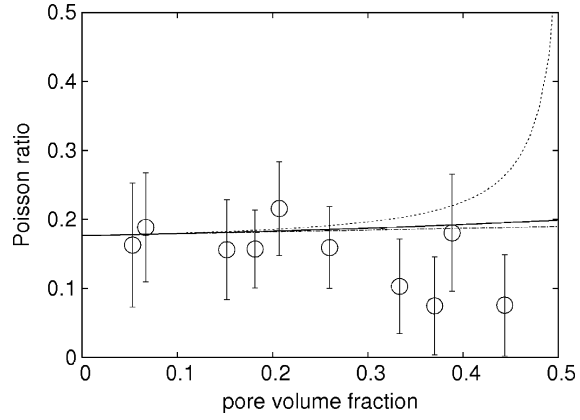

Fig. 3. The Poisson ratio vs. the pore volume fraction. Symbols and lines are the same as in Fig. 1.

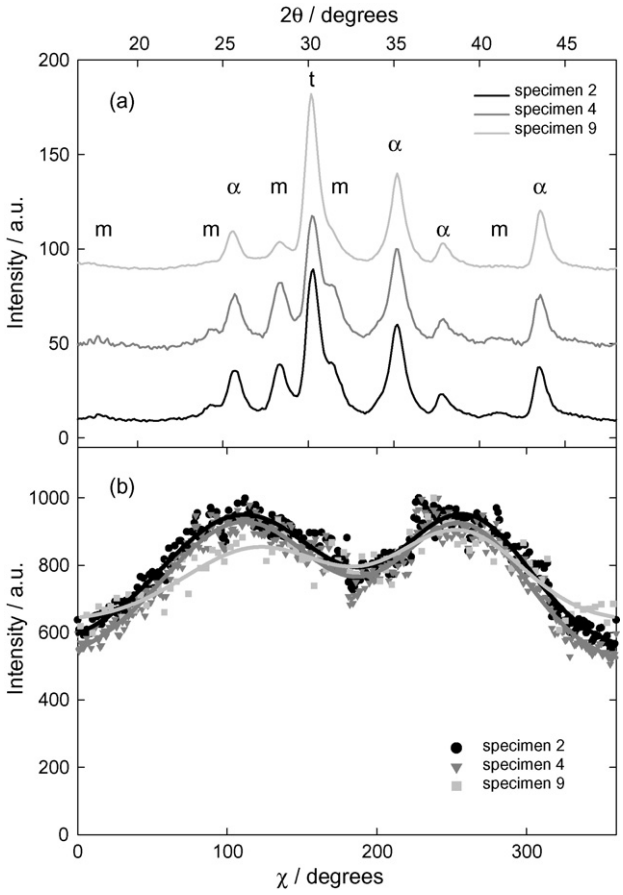

Fig. 4. X-ray diffraction data: (a) WAXD and (b) SAXS. The indices α, m and t denote the α-alumina, the monoclinic and tetragonal zirconia peaks, respectively, and the lines in Fig. 4a are vertically shifted for better visualisation of the data. (a) The intensity decrease of the monoclinic peaks shows a transition from monoclinic to tetragonal zirconia. (b) The oriented scattering in SAXS is consistent with lenticular and oriented pores.

Fig. 4 shows the wide-angle X-ray diffraction (Fig. 4a) and small-angle X-ray scattering data (Fig. 4b). For better visibility, only three specimens are shown in this figure. The peaks from α-alumina, monoclinic and tetragonal zirconia are denoted by α, m and t, respectively. The decrease of the monoclinic zirconia peak in Fig. 4a indicates a transition from monoclinic to tetragonal zirconia with increasing sintering time. The SAXS data, Fig. 4b, show scattering from oriented pores. The integrated area of the oriented and the isotropic part of the scattering curves is consistent with elliptic, lenticular pores with an aspect ratio of $\alpha = 0.66$.

Nitrogen sorption data together with the porosity of the samples are shown in Table 1. Only the first two specimens with the lowest density exhibit an open porosity, visible by the high value of the BET-surface, whereas in all other specimens the porosity is closed.

4. Discussion

With the exception of the dilute-distribution model, which is only valid if the pore volume fraction is small, the observed

Table 1
Bulk density of specimens, porosity calculated from the theoretical and the apparent densities, BET surface and pore volume, determined by nitrogen sorption

Specimen	Bulk density (g/cm^3)	Porosity	BET (m^2/g)	Total pore volume (cm^3/g)
1	2.42	0.444	399	0.359
2	2.66	0.389	11.5	0.0169
3	2.74	0.370	5.43	0.0096
4	2.90	0.333	3.36	0.0075
5	3.22	0.260	2.17	0.0049
6	3.45	0.207	1.27	0.0024
7	3.56	0.182	2.70	0.0035
8	3.69	0.152	0.46	0.0012
9	4.06	0.0667	1.47	0.0021
10	4.12	0.0529	2.98	0.0037

Only the first two specimens with the lowest bulk density have an open porosity.

decrease in the elastic properties is consistent with the theoretical predictions within the experimental error. For the Poisson ratio, Fig. 3, deviations between experiment and theory occur. This can be attributed to the high relative uncertainty of the Poisson ratio, which depends on both the Young's and the shear modulus and is calculated by subtracting 1 from a number close to 1, $\nu = E/(2G) - 1$. Despite this large uncertainty, Fig. 3 seems to confirm Dean's thesis[3] that Wu's theory overestimates the Poisson ratio for a pore volume fraction with a value higher than 0.3.

The two self-consistent theories are nearly identical within their range of validity and also in good agreement with the experimental values, whereas the differential model deviates at a much earlier point. A possible reason could be that the different models are differently sensitive to a distribution of pores, which is not perfectly isotropic. Though all models assume such an isotropy, the pores of our material exhibit a slightly preferred orientation as shown by the SAXS results. This could be a consequence of the uniaxial pressing procedure during processing. The value for the aspect ratio of the pores from SAXS ($\alpha = 0.66$) is in good coincidence with the value from the fit of the elastic data with Wu's model ($\alpha = 0.61$).

One of the basic assumptions of the different models is that the structure of the material is not altered with increasing porosity. A transition from monoclinic to tetragonal zirconia could be observed in the X-ray diffraction data, but this transition has only a minor contribution to the elastic moduli: taking a volume fraction of zirconia of $\nu_z = 0.175$ and a Young's modulus of $E_m = 230$ GPa for the monoclinic and $E_t = 211$ GPa for the tetragonal phase into account,[26] this transition has only a minor contribution to the Young's modulus, $\nu_z(E_m - E_t) = 3.3$ GPa. This might only lead to a slightly higher value for the specimens with the highest amount of monoclinic zirconia, i.e., the specimens with the highest porosity. Applying the rule of mixture to the fitted Young's modulus, $\nu_z E_r + \nu_\alpha E_\alpha = 334$ GPa, the Young's modulus for the alumina phase is $E_\alpha = 360$ GPa, which is within the range of data given in the literature,[26] however, tends towards the lower values given for dense alumina. A possible content of γ-alumina would explain this low value, but a γ-phase could not be detected in the WAXD data, Fig. 4a. Though it is generally known that it is difficult to detect γ-alumina due to the low intensity of the peaks,[27] the more probable interpretation is that the limited precision of the porosity measurements accounts for the relatively low values for the Young's modulus of the pure alumina phase.

5. Conclusion

The resonant beam technique allows the measurement of the Young's and the shear modulus of materials in an extremely wide range of porosities, which is shown for ZrO_2-toughened RBAO as an example. By removing the specimens from the sintering process at different times, porosities between nearly dense up to the limit of stability could be realized. The data can be best described with the self-consistent scheme and lenticular pores. Accompanying structural investigations by SAXS support this type of pore shape in RBAO. A transition from monoclinic to tetragonal zirconia was also observed, but it cannot account for a significant influence on the Young's modulus. Therefore, the decrease of the moduli is solely attributed to the increasing amount of porosity.

Acknowledgement

The support from the Austrian Science Funds (FWF), projects P15670 and P16315, is gratefully acknowledged.

References

1. Munro, R. G., Effective medium theory of the porosity dependence of bulk moduli. *J. Am. Ceram. Soc.*, 2001, **84**(5), 1190–1192.
2. Hagiwara, H. and Green, D. J., Elastic behaviour of open-cell alumina. *J. Am. Ceram. Soc.*, 1987, **70**(11), 811–815.
3. Dean, E. A., Elastic moduli of porous sintered materials as modeled by a variable-aspect-ratio self-consistent oblate-spheroidal-inclusion theory. *J. Am. Ceram. Soc.*, 1983, **66**(12), 847–854.
4. Wanner, A. and Kromp, K., Young's and shear moduli of laminated carbon/carbon composites by a resonant beam method. In *Brittle Matrix Composites II*, ed. A. M. Brandt and I. H. Marshall. Elsevier, England, 1989.
5. Lins, W., Kaindl, G., Peterlik, H. and Kromp, K., A novel resonant beam technique to determine the elastic moduli in dependence on orientation and temperature up to 2000 °C. *Rev. Sci. Instrum.*, 1999, **90**(7), 3052–3058.
6. Loidl, D., Puchegger, S., Kromp, K., Zeschky, J., Greil, P., Bourgeon, M. *et al.*, Elastic moduli of porous and anisotropic composites at high temperatures. *Adv. Eng. Mater.*, 2004, **6**(3), 138–142.
7. *ASTM E1875-00$^{\varepsilon 1}$—Standard Test Method for Dynamic Young's Modulus, Shear Modulus, and Poisson's Ratio by Sonic Resonance*, January 2001.
8. Phani, K. K., Porosity-dependence of elastic properties and ultrasonic velocity in polycrystalline alumina—a model based on cylindrical pores. *J. Mater. Sci.*, 1996, **31**, 262–266.
9. Gibson, L. J., Ashby, M. F., Clarke, D. R., Suresh, S. and Ward, I. M., *Cellular Solids: Structure and Properties*. Cambridge University Press, Cambridge, United Kingdom, 1997.
10. Green, D. J., Nader, C. and Brezny, R., The elastic behaviour of partially-sintered alumina. *Ceram. Transact.*, 1990, **7**, 345–356.
11. Hill, R., A self-consistent mechanics of composite materials. *J. Mech. Phys. Solids*, 1965, **13**, 213–222.
12. Budiansky, B., On the elastic moduli of some heterogeneous materials. *J. Mech. Phys. Solids*, 1965, **13**, 223–227.
13. Wu, T. T., The effect of inclusion shape on the elastic moduli of a two-phase material. *Int. J. Sol. Struct.*, 1966, **2**, 1–8.

14. Berryman, J. G., Long-wavelength propagation in composite elastic media. II. Ellipsoidal inclusions. *J. Acoust. Soc. Am.*, 1980, **68**(6), 1820–1831.
15. Nemat-Nasser, S. and Hori, M., *Micromechanics: Overall Properties of Heterogeneous Materials* (*2nd ed.*). Elsevier, The Netherlands, 1999.
16. Roscoe, R., Isotropic composites with elastic and viscoelastic phases: general bounds for the moduli and solutions for special geometries. *Rheol. Acta*, 1973, **12**, 404–411.
17. Eshelby, J. D., The determination of the elastic field of an ellipsoidal inclusion, and related problems. *Proc. Royal Soc.*, 1957, **241**, 376–396.
18. Claussen, N., Le, T. and Wu, S., Low-shrinkage reaction-bonded alumina. *J. Eur. Ceram. Soc.*, 1989, **5**, 29–35.
19. Claussen, N., Travitzky, N. A. and Wu, S., Tailoring of reaction-bonded Al_2O_3 RBAO ceramics. *Ceram. Eng. Sci. Proc.*, 1990, **11**, 806–820.
20. Claussen, N., Wu, S. and Holz, D., Reaction bonding of aluminum oxide (RBAO) composites: processing, reaction mechanisms and properties. *J. Eur. Ceram. Soc.*, 1994, **14**, 97–109.
21. Timoshenko, S. P., On the correction for shear of the differential equation for transverse vibrations of prismatic bars. *Phil. Mag.*, 1921, **41**, 744–746.
22. Timoshenko, S. P., On the transverse vibrations of bars of uniform cross-section. *Phil. Mag.*, 1922, **43**, 125–131.
23. Burgholzer, P., Hofer, C., Reitinger, B., Mohammed, A., Degischer, H. P., Loidl, D. *et al.*, Non-contacting determination of elastic moduli of continuous fiber reinforced metals. *Comp. Sci. Technol.*, 2005, **65**(2), 301–306.
24. Puchegger, S., Bauer, S., Loidl, D., Kromp, K. and Peterlik, H., Experimental validation of the shear correction factor. *J. Sound Vib.*, 2003, **261**, 177–184.
25. Leisure, R. G. and Willis, F. A., Resonant ultrasound spectroscopy. *J. Phys. Condens. Matter*, 1997, **9**, 6001–6029 [NIST Standard Reference Database #30, Version: April 2003].
26. NIST Standard Reference Database #30, Version: April 2003.
27. Wu, S. X., Holz, D. and Claussen, N., Mechanisms and kinetics of reaction-bonded aluminum oxide ceramics. *J. Am. Ceram. Soc.*, 1993, **76**(4), 970–980.